



Published in final edited form as:

Stroke Vasc Interv Neurol. 2022 July ; 2(4): . doi:10.1161/svin.121.000309.

Topographical Analysis of Aneurysm Wall Enhancement With 3-Dimensional Mapping

Ashrita Raghuram, BSE¹, Alberto Varon, MD¹, Sebastian Sanchez, MD¹, Daizo Ishii, MD², Chaorong Wu, PhD³, Vincent A Magnotta, PhD⁴, David M. Hasan, MD⁶, Timothy R. Kosciak, PhD⁵, Edgar A. Samaniego, MD, MS^{1,2,4}

¹Department of Neurology, University of Iowa Carver College of Medicine, Iowa City, IA.

²Department of Neurosurgery, University of Iowa Carver College of Medicine, Iowa City, IA.

³Institute for Clinical and Translational Science, University of Iowa, Iowa City, IA.

⁴Department of Radiology, University of Iowa Carver College of Medicine, Iowa City, IA.

⁵Department of Psychiatry, University of Iowa Carver College of Medicine, Iowa City, IA.

⁶Department of Neurosurgery, Duke University, Durham, NC

Abstract

Background: Aneurysm wall enhancement has been identified as a potential biomarker for aneurysm instability. Enhancement has been determined by different approaches on 2D multiplanar views. This study describes a new method to quantify enhancement through 3D heatmaps and histograms.

Methods: A custom algorithm was developed using orthogonal probes extending from the aneurysm lumen into the wall to create 3D heatmaps and histograms of wall enhancement on 7T-MRI. Three quantitative metrics for general, specific, and focal wall enhancement were generated from the histograms.

Results: Thirty-two aneurysms were analyzed and classified based on 3D heatmaps and histograms. Larger aneurysms were more enhancing (Spearman's $r=0.472$, $p=0.006$), and had more heterogeneous enhancement (Spearman's $r=0.557$, $p<0.001$) than smaller aneurysms. Patterns of enhancement differed between saccular, fusiform, and thrombosed aneurysms. Fusiform aneurysms were larger ($p=0.015$) and had more heterogeneous enhancement compared to saccular aneurysms. Fusiform aneurysms had more areas of focal enhancement ($p<0.001$) and right skewed histograms ($p=0.003$).

Corresponding Author: Edgar A Samaniego MD, MS, Associate Professor of Neurology, Neurosurgery and Radiology, 200 Hawkins Drive, Iowa City, Iowa 52246, United States of America, 319-333-4460, edgarsama@gmail.com.

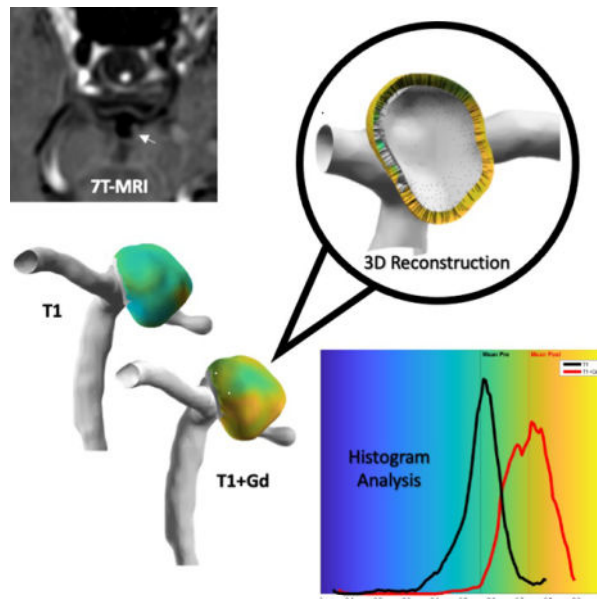
Contributions: Conception and study design: EAS; acquisition of data: AR, AV, TRK; analysis and interpretation of results: AR, AV, WC, TRK and EAS; drafting of the manuscript: AR and EAS; critical revision of the study: all authors; final approval of the version to be published: TRK and EAS.

DISCLOSURES: none.

SUPPLEMENTAL MATERIAL: Supplementary Tables S1 and S2

Conclusions: The 3D analysis of aneurysm wall enhancement provides topographic data of the entire aneurysm wall. New metrics developed based on this method showed that large and fusiform aneurysms have heterogenous enhancement.

Graphical Abstract



INTRODUCTION:

Aneurysm wall enhancement (AWE) has been described as a potential biomarker for aneurysm growth and rupture.^{1,2} Aneurysms are complex vascular structures that undergo heterogeneous biological processes. Histological analysis of the aneurysm wall has revealed a multifaceted process of de-endothelization, thrombosis, proliferation, apoptosis and leukocyte infiltration.^{3,4} AWE after the administration of contrast gadolinium (Gd) may be used as a surrogate biomarker of some of these biological processes.^{5,6}

High-resolution MRI (HR-MRI) can provide insights into the vessel wall not seen on conventional imaging and has been used to characterize AWE. However, there is a lack of consensus on which specific patterns of AWE predict aneurysm instability. Most methods for assessing enhancement rely on subjective analysis. This approach is sub-optimal as it not based on objective metrics and introduces bias. Some studies described the presence of circumferential AWE (CAWE) as a marker of unstable aneurysms, while others have described positive correlations between focal AWE (FAWE) and known predictors of instability.^{7,8} Other studies have determined that symptomatic aneurysms have increased AWE between pre and post-contrast imaging.⁹ The wide-range of definitions of enhancement limit the reproducibility of results and make comparisons challenging.

The comprehensive analysis of AWE would require the characterization of both regional and global changes within the aneurysm wall. So far, the study of AWE has been limited to 2D multiplanar views, diminishing the visualization of these complex 3D structures. In

this study, we propose a new qualitative and quantitative 3D method of assessing AWE. We used the high-resolution of 7T-MRI as a platform to develop high-fidelity 3D reconstructions and generate 3D-AWE maps of the entire wall. This innovative approach aims at providing a thorough assessment of the whole aneurysm using a new set of quantitative metrics.

METHODS:

Semi-Automatic Quantification of Enhancement and 3D-AWE Reconstruction:

The data that supports the findings of this study are available from the corresponding author upon reasonable request. After institutional review board approval, patients with unruptured intracranial aneurysms underwent HR-MRI on a GE 7T MRI (Discovery MR950) from August 2018 to December 2020. (Supplementary Table S1). Using a previously described method for 3D-AWE quantification, manual segmentations of the aneurysm sac were created from registered T1 and T1+Gd images.¹⁰ Spokes were extended outwards orthogonal to the surface to probe the aneurysm wall. The spoke length was determined by a distance equivalent to the average radiological wall thickness measured on T1+Gd imaging. The signal intensity (SI) value of each spoke was collected for analysis and normalized to the genu of the corpus callosum (CC):

$$CC_{ratio} = SI_{max\ spoke} / SI_{mean\ CC}$$

These values were subsequently mapped to the aneurysm surface to create 3D-AWE heatmaps.

Histograms of the AWE data were created over 100 bins for T1 and T1+Gd reconstructions. Histogram shape was characterized using skewness, kurtosis, and standard deviation (σ).¹⁰

Classifications of AWE:

The circumferential SI (μ) was calculated by averaging the values from each spoke over the entire aneurysm surface. This would be equivalent to the 2D-CAWE described by other authors. Circumferential SI was used to generate T1 and T1+Gd 3D reconstructions.

$$Circumferential\ SI: \mu = \sum CC_{ratio} / N_{spokes}$$

Specific aneurysm wall enhancement (SAWE) was used to describe the dynamic uptake of contrast between T1 and T1+Gd imaging. SAWE+ aneurysms were defined as having greater than two standard deviations (SDs) of circumferential SI on T1+Gd when compared to T1 ($\mu_{post} - \mu_{pre} + 2\sigma$).

$$\begin{cases} SAWE+: \mu_{post} \geq \mu_{pre} + 2\sigma_{pre} \\ SAWE-: \mu_{post} < \mu_{pre} + 2\sigma_{pre} \end{cases}$$

General aneurysm wall enhancement (GAWE) was used to characterize enhancement relative to the entire cohort based only on T1+Gd imaging. Aneurysms with an enhancement ratio higher than the CC ($\mu_{post} - 1$) were classified as GAWE+. Previous studies have

established different thresholds after normalization.¹¹ In this analysis we used a μ_{post} 1 as a threshold for enhancement.

$$\begin{cases} GAWE+ : \mu_{post} \geq 1 \\ GAWE- : \mu_{post} < 1 \end{cases}$$

Lastly, focal aneurysm wall enhancement (FAWE) was used as a measure of regional/focal enhancement when compared to the rest of the aneurysm. Spokes with a CC_{ratio} greater than 2 SDs above the circumferential SI of the T1+Gd reconstruction were considered FAWE+ ($CC_{ratio} \mu_{post} + 2\sigma$). Areas of FAWE were determined by the density of spokes above this threshold.

$$\begin{cases} FAWE+ : CC \text{ Ratio} \geq \mu_{post} + 2\sigma_{post} \\ FAWE- : CC \text{ Ratio} < \mu_{post} + 2\sigma_{post} \end{cases}$$

Measurements of Aneurysm Morphology:

Fusiform aneurysms were defined as an arterial dilation greater than 1.5 times normal without a clearly definable neck.¹² Size ratio and aspect ratio were measured as defined by Dhar et al.¹³ Mural/intrasaccular thrombosis was identified as high T1 signal, or isointense signal to the normal vessel wall.¹⁴

Statistical Analysis:

All statistical analysis was conducted using SPSS Statistics 27 (IBM, New York, USA). Categorical variables are presented as frequency and percentage, and continuous variables as mean \pm SD. All statistical tests used two-tail alternatives and assessed significance at $\alpha = 0.05$. Paired categorical data was compared using McNemar's Test. The Shapiro-Wilk test for normality was used to identify normally distributed continuous variables. Normally distributed continuous data were compared using an independent Student's t-test, and non-normally distributed data were compared using a Mann-Whitney U-Test. Comparisons between multiple groups were conducted using a one-way ANOVA with a Tukey post hoc test. Pearson correlations were used to evaluate the linear relationship between normally distributed variables and Spearman correlations were used to evaluate relationships involving non-normally distributed variables.

RESULTS:

Enhancement Metrics:

A total of 32 aneurysms were included in the analysis: 24 saccular and 8 fusiform. Two fusiform (6.25%) aneurysms had mural/saccular thrombosis. Demographic and location data are available in Supplementary Table S2. Ten (31.25%) aneurysms were classified as GAWE+ and 14 (43.75%) as SAWE+. Eight (25%) aneurysms met both criteria for enhancement (GAWE+/SAWE+), while sixteen (50%) aneurysms did not meet any criteria for enhancement (GAWE-/SAWE-). GAWE+/SAWE+ saccular aneurysms were larger in size and had higher size and aspect ratios compared to GAWE-/SAWE- aneurysms.

(Table 1). Enhancing aneurysms were often found in locations associated with high risk of rupture (anterior communicating artery, posterior communicating artery, basilar artery, and posterior-inferior cerebellar artery): 67% GAWE+, 55% SAWE+ and 67% GAWE+/SAWE+.

Histogram Shape Metrics in Large Aneurysms:

Larger aneurysms (> 7 mm, N=14) had significantly higher circumferential SI compared to smaller aneurysms (N=18) on both T1 and T1+Gd reconstructions ($p<0.001$ and $p=0.034$ respectively). Larger aneurysms also had significantly higher SDs (histogram width) for T1 and T1+Gd reconstructions ($p<0.001$ and $p=0.022$ respectively). Lastly, larger aneurysms had less negative (left) skew compared to smaller aneurysms on T1 ($p=0.002$) and T1+Gd histograms ($p=0.068$). Positively skewed histograms had larger areas of FAWE and wider histograms. Skewness was correlated with area of FAWE (Spearman $r=0.871$, $p<0.001$) and histogram SD (Pearson $r=0.510$, $p=0.003$).

Patterns of Enhancement in Fusiform and Thrombosed Aneurysms:

Saccular and fusiform aneurysms displayed different patterns of enhancement. (Table 2). Four (50%) out of the eight fusiform aneurysms were GAWE+ and three (37.5%) were SAWE+. Two (25%) aneurysms were GAWE+/SAWE+, and three (37.5%) were GAWE-/SAWE-. The threshold to define SAWE was higher ($p=0.006$) in fusiform ($\mu=1.09$) than saccular aneurysms ($\mu=0.82$). All fusiform and 19 saccular aneurysms (79.2%) displayed areas of focal enhancement. Fusiform aneurysms were larger in size, had thicker walls and had more heterogeneous surface enhancement when compared to saccular aneurysms (Figure 1B and 2B). Two fusiform (25%) had mural/saccular thrombosis. Some aneurysms with extensive thrombosis had more avid luminal wall enhancement on T1 than T1+Gd imaging and were SAWE- (Figure 3). Both thrombosed aneurysms showed subsequent changes in size/luminal area on follow-up and were therefore considered unstable.

DISCUSSION:

The quantitative data obtained from 3D AWE mapping provides a comprehensive analysis of aneurysm enhancement. Histogram shape metrics, such as skewness and SD provide information about regional enhancement within each aneurysm. 3D-AWE mapping encompasses the entire wall in all dimensions and allows identification of subtle enhancement differences that may reflect different biological processes of the aneurysm wall.

Histogram Shape Metrics in Large Aneurysms:

The histogram width represents the distribution of enhancement along the entire aneurysm. A larger aneurysm may have more dispersion of enhancement as the wall may undergo different biological process in different compartments. The skewness of the distribution can be used to represent the increased concentration of wall enhancement towards low or high SI. Large areas of focal enhancement located in the right tail of the histogram create a right and positive skew. Aneurysms that exhibited common features of instability (size >7 mm, aspect ratio >1.3 and size ratio >3) had different histogram shapes compared

to stable aneurysms.^{15–18} Larger aneurysms (> 7 mm) had broader and right-positive skewed histograms, compared to smaller aneurysms. The identification of this pattern of enhancement in smaller aneurysms in a larger sample size may allow the identification of small unstable aneurysms. This is a common paradigm in anterior communicating aneurysms which tend to be smaller at the time of rupture.¹⁹

Histogram Shape Metrics in Fusiform Aneurysms:

The quantification of different enhancement patterns through the analysis of histogram shape metrics established clear differences between saccular and fusiform aneurysms (Table 2). Fusiform aneurysms had higher circumferential SI on T1+Gd imaging and larger areas of focal enhancement, leading to wider, and positively skewed histograms compared to saccular aneurysms (Figure 2). 3D-AWE maps demonstrated a more heterogenous distribution of enhancement in fusiform aneurysms compared to saccular aneurysms. Fusiform aneurysms also exhibited regional enhancement along the aneurysm body. Thicker walls, larger size and more areas of focal enhancement (an average of 3 versus 1 in saccular aneurysms) highly suggest that fusiform aneurysms form and grow due to unique biological processes, as opposed to saccular aneurysms.^{20–22}

General Aneurysm Wall Enhancement (GAWE):

A normalized metric for AWE is necessary to compare enhancement between different aneurysms. We previously established an AWE cutoff normalized to the pituitary stalk ($CR_{\text{stalk}}=0.60$) in identifying aneurysms > 7 mm.²³ However, this approach was also bounded to manual ROIs determined on 2D imaging. The pituitary stalk avidly enhances on T1+Gd imaging and introduces artifact into the quantification of AWE.¹⁰ Therefore, in the current analysis we used the CC for normalization. The quantification of the degree of enhancement relative to the CC on T1+Gd imaging, is equivalent to the AWE cutoff of 0.60 determined in previous studies. In the current analysis, any aneurysm that enhanced more than the CC ($\mu_{\text{post}} - 1$) was classified as GAWE+. Ten out of 32 aneurysms in our cohort met this criterion. These aneurysms were larger in size and had higher aspect and size ratios. (Table 1). It is yet to be determined in a larger cohort whether a better threshold would be more accurate in detecting unstable aneurysms.

Specific Aneurysm Wall Enhancement (SAWE):

Comparing changes in circumferential SI before and after contrast administration allows for the quantification of aneurysmal Gd uptake. SAWE is an aneurysm specific metric used to quantify contrast uptake by comparing T1 and T1+Gd reconstructions. Omodaka et al defined wall enhancement index as the change in enhancement between T1 and T1+Gd images.²⁴ This index predicted aneurysm rupture with a sensitivity of 100% and specificity of 69%.²⁵ We classified SAWE+ aneurysms as the ones that had substantial increase (2SDs) in circumferential SI after contrast administration ($\mu_{\text{post}} - \mu_{\text{pre}} + 2\sigma_{\text{pre}}$). In our cohort, saccular aneurysms with uniform AWE distributions were classified as SAWE+, even though they appeared subjectively non-enhancing on T1+Gd imaging (Figure 1). Fusiform aneurysms with heterogeneous AWE distribution could also be classified as SAWE+ after substantial contrast uptake (Figure 2). The method described in this study allows to gauge in detail the amount of enhancement exhibited by each aneurysm and by a particular segment

of the aneurysm. In a saccular aneurysm, about 82% of spokes enhanced above the SAWE threshold, while only 2.5% showed focal enhancement. (Figure 1D). Conversely, a fusiform aneurysm showed a similar broad uptake of contrast with 71% of spokes enhancing above the SAWE cutoff in addition to a larger (4%) area of focal enhancement. (Figure 2D). SAWE has the potential of translating different phenomena among different types of aneurysms. Saccular aneurysms are more likely to show uniform patterns of enhancement, whereas fusiform aneurysms are more likely to show focal heterogeneous patterns of enhancement. Aneurysms with significant heterogeneity on pre-contrast imaging, suggestive of complex vascular processes such as the presence of mural thrombosis, may not be classified as SAWE+ due to inherent enhancement on T1 imaging. (Figure 3)

Focal Aneurysm Wall Enhancement (FAWE):

Areas of focal enhancement (FAWE) have been correlated with areas of instability, bleb formation and higher risk of rupture. Our previous comparison of the enhancement patterns in aneurysms with blebs showed that 53% of the aneurysms with blebs had increased enhancement in the bleb (8%) as compared to the sac.¹⁰ Larsen et al reported colocalization of such areas with hemodynamic parameters predictive of aneurysm rupture.⁷ Khan et al also co-localized AWE to areas of low wall shear stress (WSS).²⁶ It is challenging to determine the presence of FAWE on 2D multiplanar images. In our study, we visualized FAWE on 3D-AWE maps and determined the density of FAWE on T1+Gd reconstructions. By comparing the CC_{ratio} of individual spokes relative to the aneurysm body, the area of focal enhancement could be objectively identified. Spokes that substantially enhanced ($>2SDs$) compared to the circumferential SI on T1+Gd were considered FAWE+ ($CC_{ratio} > \mu_{post} + 2\sigma_{post}$). By identifying the density of spokes in the heatmap that met this criterion, we identified if there were multiple areas of focal enhancement in the same aneurysm (Figure 2D). Cebra et al reported regional aneurysm wall changes associated with rupture points and instability.²⁷ Similarly, Ashkezari et al demonstrated that spatial variations in hemodynamic parameters such as WSS may have a relationship with bleb location and rupture points.²⁸ FAWE could potentially identify such areas that may be susceptible to rupture.²⁹ FAWE can be identified both qualitatively in 3D heatmaps and quantitatively using T1+Gd histograms. FAWE also represents the heterogeneous patterns of enhancement that may be present in different biological processes such as atherosclerosis, proliferation of vasa vasorum and/or slow flow conditions. Fusiform aneurysms had more areas of FAWE than saccular aneurysms.

Patterns of AWE in Thrombosed Aneurysms:

Thrombosed aneurysms exhibited specific patterns of enhancement that suggest different patterns of Gd penetration in the aneurysm structures. In the thrombosed vertebrobasilar aneurysm, AWE was very heterogeneous in the outer and thrombosed wall, while the inner wall closest to the patent lumen exhibited uniform enhancement (Figure 3A–B). Contrast dynamics in these complex structures translated into changes in areas of FAWE between T1 and T1+Gd imaging (Figure 3C). We hypothesize that the intramural thrombus limits the uptake of Gd by the outer thrombosed wall and prevents the detection of SAWE. Matsushige et al paired histological aneurysm analysis with focal enhancement and suggested that the organization of fresh intraluminal thrombus into a loose matrix allowed for thrombus to

retain contrast media.³⁰ This may explain why these aneurysms are SAWE– and GAWE+. Sato et al characterized the double-rim wall enhancement visible on 7T-MRI of thrombosed aneurysms as neovascularization of the inner wall layer adjacent to thrombus and vasa vasorum in the outer wall layer.³¹ This pattern is consistent with our results showing that focal enhancement may be associated with areas of thrombosis that create complex patterns of enhancement on both T1 and T1+Gd imaging (Figure 3A–B). Quantitative metrics derived from 3D AWE maps and histogram analysis of the outer wall allow identification of these aneurysms. Increases in skewness or changes in histogram SD after contrast administration most likely reflect the complex pattern of contrast retention in these thrombosed regions.

Limitations:

This study is limited by the small sample size and by the heterogeneity of aneurysms selected for analysis. While we identified trends in AWE metrics compared to known predictors for instability, the small sample size limited the generalizability and statistical power of the analysis. The study was performed with a 7T MRI platform, which does not have clinical use. However, by developing this method with high resolution 7T-MRI, we optimized a framework for larger 3T MRI analyses. 7T-MRI allows for clear identification of the aneurysm wall, but wall thickness was measured radiologically, which may have included artifact from “leaky” Gd. Additionally, this method allowed automated generation of 3D heat maps. However, manual labeling was required for aneurysm segmentation and quality checks. Further work is needed to create a fully automated tool for clinical use.

CONCLUSIONS:

3D-AWE mapping paired with histogram analysis provides numerous new qualitative and quantitative metrics for aneurysm analysis.

Supplementary Material

Refer to Web version on PubMed Central for supplementary material.

SOURCES OF FUNDING:

This work was conducted on an MRI instrument funded by 1S10RR028821-01. This study was supported in part by the University of Iowa Institute for Clinical and Translational Science, which is granted with Clinical and Translational Science Award funds from the National Institutes of Health (UL1TR002537).

Abbreviations:

HR-MRI	High Resolution MRI
SI	Signal Intensity
Gd	Gadolinium
T1+Gd	T1 Weighted Post Gadolinium Contrast MRI
CC	Corpus Callosum

AWE	Aneurysm Wall Enhancement
CAWE	Circumferential Aneurysm Wall Enhancement
FAWE	Focal Aneurysm Wall Enhancement
GAWA	General Aneurysm Wall Enhancement
SAWE	Specific Aneurysm Wall Enhancement

REFERENCES:

- Larson AS, Lehman VT, Lanzino G, Brinjikji W. Lack of Baseline Intracranial Aneurysm Wall Enhancement Predicts Future Stability: A Systematic Review and Meta-Analysis of Longitudinal Studies. *AJNR Am J Neuroradiol*. 2020;41:1606–1610. doi: 10.3174/ajnr.A6690 [PubMed: 32819901]
- Samaniego EA, Roa JA, Hasan D. Vessel wall imaging in intracranial aneurysms. *J Neurointerv Surg*. 2019;11:1105–1112. doi: 10.1136/neurintsurg-2019-014938 [PubMed: 31337731]
- Frosen J, Piippo A, Paetau A, Kangasniemi M, Niemela M, Hernesniemi J, Jaaskelainen J. Remodeling of saccular cerebral artery aneurysm wall is associated with rupture: histological analysis of 24 unruptured and 42 ruptured cases. *Stroke*. 2004;35:2287–2293. doi: 10.1161/01.STR.0000140636.30204.da [PubMed: 15322297]
- Hudson JS, Zanaty M, Nakagawa D, Kung DK, Jabbour P, Samaniego EA, Hasan D. Magnetic Resonance Vessel Wall Imaging in Human Intracranial Aneurysms. *Stroke*. 2018;STROKEAHA118023701. doi: 10.1161/STROKEAHA.118.023701
- Portanova A, Hakakian N, Mikulis DJ, Virmani R, Abdalla WM, Wasserman BA. Intracranial vasa vasorum: insights and implications for imaging. *Radiology*. 2013;267:667–679. doi: 10.1148/radiol.13112310 [PubMed: 23704290]
- McDonald RJ, McDonald JS, Kallmes DF, Jentoft ME, Murray DL, Thielen KR, Williamson EE, Eckel LJ. Intracranial Gadolinium Deposition after Contrast-enhanced MR Imaging. *Radiology*. 2015;275:772–782. doi: 10.1148/radiol.15150025 [PubMed: 25742194]
- Larsen N, Fluh C, Saalfeld S, Voss S, Hille G, Trick D, Wodarg F, Synowitz M, Jansen O, Berg P. Multimodal validation of focal enhancement in intracranial aneurysms as a surrogate marker for aneurysm instability. *Neuroradiology*. 2020;62:1627–1635. doi: 10.1007/s00234-020-02498-6 [PubMed: 32681192]
- Edjlali M, Guedon A, Ben Hassen W, Boulouis G, Benzakoun J, Rodriguez-Regent C, Trystram D, Nataf F, Meder JF, Turski P, et al. Circumferential Thick Enhancement at Vessel Wall MRI Has High Specificity for Intracranial Aneurysm Instability. *Radiology*. 2018;289:181–187. doi: 10.1148/radiol.2018172879 [PubMed: 29969070]
- Zhu C, Wang X, Eisenmenger L, Shi Z, Degnan A, Tian B, Liu Q, Hess C, Saloner D, Lu J. Wall enhancement on black-blood MRI is independently associated with symptomatic status of unruptured intracranial saccular aneurysm. *Eur Radiol*. 2020;30:6413–6420. doi: 10.1007/s00330-020-07063-6 [PubMed: 32666320]
- Raghuram A, Varon A, Roa JA, Ishii D, Lu Y, Raghavan ML, Wu C, Magnotta VA, Hasan DM, Kosciak TR, et al. Semiautomated 3D mapping of aneurysmal wall enhancement with 7T-MRI. *Sci Rep*. 2021;11:18344. doi: 10.1038/s41598-021-97727-0 [PubMed: 34526579]
- Roa JA, Zanaty M, Osorno-Cruz C, Ishii D, Bathla G, Ortega-Gutierrez S, Hasan D, Samaniego EA. Objective quantification of contrast enhancement of unruptured intracranial aneurysms: a high-resolution vessel wall imaging validation study. *J Neurosurg*. 2020. doi: 10.3171/2019.12.JNS192746
- Flemming KD, Wiebers DO, Brown RD Jr., Link MJ, Huston J 3rd, McClelland RL, Christianson TJ. The natural history of radiographically defined vertebrobasilar nonsaccular intracranial aneurysms. *Cerebrovasc Dis*. 2005;20:270–279. doi: 10.1159/000087710 [PubMed: 16123548]
- Dhar S, Tremmel M, Mocco J, Kim M, Yamamoto J, Siddiqui AH, Hopkins LN, Meng H. Morphology parameters for intracranial aneurysm rupture risk assessment. *Neurosurgery*.

- 2008;63:185–196; discussion 196–187. doi: 10.1227/01.NEU.0000316847.64140.81 [PubMed: 18797347]
14. Krings T, Alvarez H, Reinacher P, Ozanne A, Baccin CE, Gandolfo C, Zhao WY, Reinges MH, Lasjaunias P. Growth and rupture mechanism of partially thrombosed aneurysms. *Interv Neuroradiol.* 2007;13:117–126. doi: 10.1177/159101990701300201 [PubMed: 20566139]
 15. Investigators UJ, Morita A, Kirino T, Hashi K, Aoki N, Fukuhara S, Hashimoto N, Nakayama T, Sakai M, Teramoto A, et al. The natural course of unruptured cerebral aneurysms in a Japanese cohort. *N Engl J Med.* 2012;366:2474–2482. doi: 10.1056/NEJMoa1113260 [PubMed: 22738097]
 16. Wiebers DO, Whisnant JP, Huston J 3rd, Meissner I, Brown RD Jr., Piepgras DG, Forbes GS, Thielen K, Nichols D, O'Fallon WM, et al. Unruptured intracranial aneurysms: natural history, clinical outcome, and risks of surgical and endovascular treatment. *Lancet.* 2003;362:103–110. doi: 10.1016/s0140-6736(03)13860-3 [PubMed: 12867109]
 17. Backes D, Vergouwen MD, Velthuis BK, van der Schaaf IC, Bor AS, Algra A, Rinkel GJ. Difference in aneurysm characteristics between ruptured and unruptured aneurysms in patients with multiple intracranial aneurysms. *Stroke.* 2014;45:1299–1303. doi: 10.1161/STROKEAHA.113.004421 [PubMed: 24652309]
 18. Rahman M, Smietana J, Hauck E, Hoh B, Hopkins N, Siddiqui A, Levy EI, Meng H, Mocco J. Size ratio correlates with intracranial aneurysm rupture status: a prospective study. *Stroke.* 2010;41:916–920. doi: 10.1161/STROKEAHA.109.574244 [PubMed: 20378866]
 19. Lee JY, Seo JH, Cho YD, Kang HS, Han MH. Endovascular Treatment of 429 Anterior Communicating Artery Aneurysms Using Bare-Platinum Coils : Clinical and Radiologic Outcomes at the Long-term Follow-up. *J Korean Neurosurg Soc.* 2015;57:159–166. doi: 10.3340/jkns.2015.57.3.159 [PubMed: 25810854]
 20. Park SH, Yim MB, Lee CY, Kim E, Son EI. Intracranial Fusiform Aneurysms: It's Pathogenesis, Clinical Characteristics and Managements. *J Korean Neurosurg Soc.* 2008;44:116–123. doi: 10.3340/jkns.2008.44.3.116 [PubMed: 19096660]
 21. Sabotin RP, Varon A, Roa JA, Raghuram A, Ishii D, Nino M, Galloy AE, Patel D, Raghavan ML, Hasan D, et al. Insights into the pathogenesis of cerebral fusiform aneurysms: high-resolution MRI and computational analysis. *J Neurointerv Surg.* 2021. doi: 10.1136/neurintsurg-2020-017243
 22. Liu X, Zhang Z, Zhu C, Feng J, Liu P, Kong Q, Zhang X, Zhang Q, Jin H, Ge H, et al. Wall enhancement of intracranial saccular and fusiform aneurysms may differ in intensity and extension: a pilot study using 7-T high-resolution black-blood MRI. *Eur Radiol.* 2020;30:301–307. doi: 10.1007/s00330-019-06275-9 [PubMed: 31218429]
 23. Roa JA, Zanaty M, Osorno-Cruz C, Ishii D, Bathla G, Ortega-Gutierrez S, Hasan DM, Samaniego EA. Objective quantification of contrast enhancement of unruptured intracranial aneurysms: a high-resolution vessel wall imaging validation study. *J Neurosurg.* 2020;134:862–869. doi: 10.3171/2019.12.JNS192746 [PubMed: 32032948]
 24. Omodaka S, Endo H, Niizuma K, Fujimura M, Inoue T, Sato K, Sugiyama SI, Tominaga T. Quantitative Assessment of Circumferential Enhancement along the Wall of Cerebral Aneurysms Using MR Imaging. *AJNR Am J Neuroradiol.* 2016;37:1262–1266. doi: 10.3174/ajnr.A4722 [PubMed: 26939634]
 25. Omodaka S, Endo H, Niizuma K, Fujimura M, Inoue T, Endo T, Sato K, Sugiyama SI, Tominaga T. Circumferential wall enhancement in evolving intracranial aneurysms on magnetic resonance vessel wall imaging. *J Neurosurg.* 2018:1–7. doi: 10.3171/2018.5.JNS18322
 26. Khan MO, Toro Arana V, Rubbert C, Cornelius JF, Fischer I, Bostelmann R, Mijderwijk HJ, Turowski B, Steiger HJ, May R, et al. Association between aneurysm hemodynamics and wall enhancement on 3D vessel wall MRI. *J Neurosurg.* 2020:1–11. doi: 10.3171/2019.10.JNS191251
 27. Cebal JR, Detmer F, Chung BJ, Choque-Velasquez J, Rezai B, Lehto H, Tulamo R, Hernesniemi J, Niemela M, Yu A, et al. Local Hemodynamic Conditions Associated with Focal Changes in the Intracranial Aneurysm Wall. *AJNR Am J Neuroradiol.* 2019;40:510–516. doi: 10.3174/ajnr.A5970 [PubMed: 30733253]
 28. Salimi Ashkezari SF, Mut F, Chung BJ, Yu AK, Stapleton CJ, See AP, Amin-Hanjani S, Charbel FT, Rezai Jahromi B, Niemela M, et al. Hemodynamics in aneurysm blebs with different wall characteristics. *J Neurointerv Surg.* 2021;13:642–646. doi: 10.1136/neurintsurg-2020-016601 [PubMed: 33020208]

29. Hashimoto Y, Matsushige T, Shimonaga K, Hosogai M, Kaneko M, Ono C, Mizoue T. Vessel Wall Imaging Predicts the Presence of Atherosclerotic Lesions in Unruptured Intracranial Aneurysms. *World Neurosurg.* 2019;132:e775–e782. doi: 10.1016/j.wneu.2019.08.019 [PubMed: 31415889]
30. Matsushige T, Shimonaga K, Mizoue T, Hosogai M, Hashimoto Y, Kaneko M, Ono C, Ishii D, Sakamoto S, Kurisu K. Focal Aneurysm Wall Enhancement on Magnetic Resonance Imaging Indicates Intraluminal Thrombus and the Rupture Point. *World Neurosurg.* 2019;127:e578–e584. doi: 10.1016/j.wneu.2019.03.209 [PubMed: 30928597]
31. Sato T, Matsushige T, Chen B, Gembruch O, Dammann P, Jabbarli R, Forsting M, Junker A, Maderwald S, Quick HH, et al. Wall Contrast Enhancement of Thrombosed Intracranial Aneurysms at 7T MRI. *AJNR Am J Neuroradiol.* 2019;40:1106–1111. doi: 10.3174/ajnr.A6084 [PubMed: 31147351]

Clinical Perspective:

- A novel semi-automated method developed with high-resolution 7T MRI, allows a detailed topographic analysis of aneurysm wall enhancement after the administration of gadolinium.
- Fusiform and large saccular aneurysms have a very heterogenous pattern of enhancement suggestive of complex biological processes within the aneurysm wall.

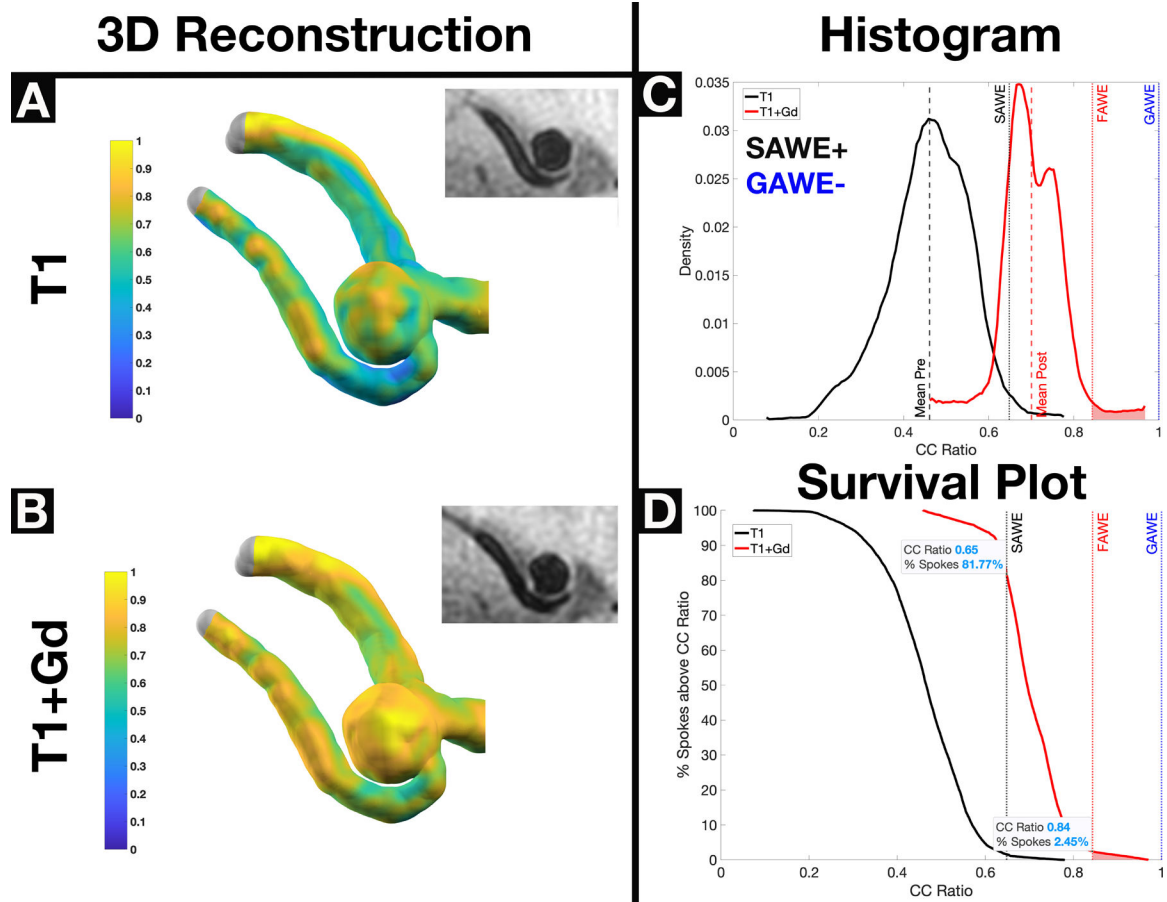
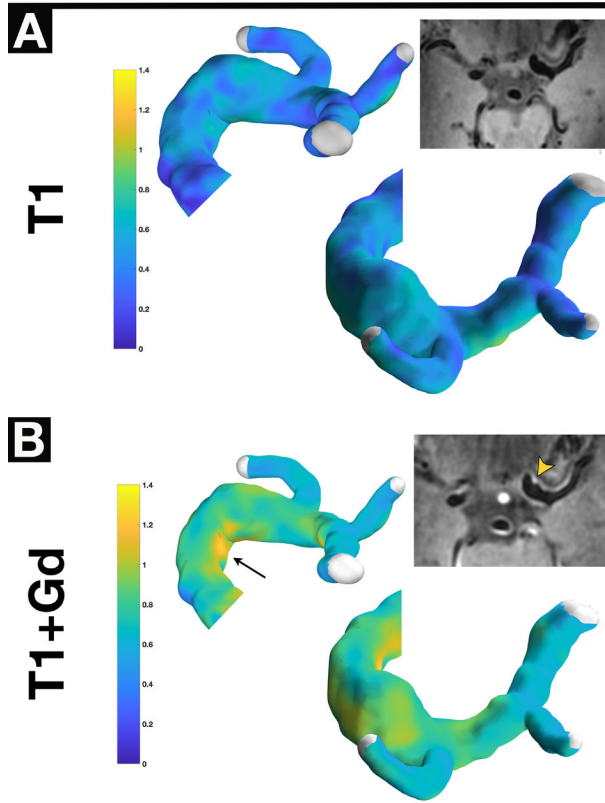


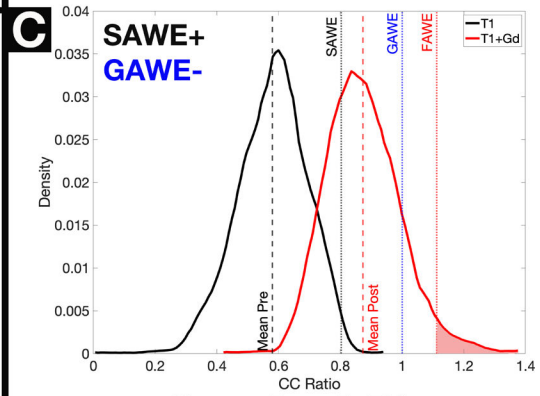
Figure 1.

A saccular GAWE–/SAWE+ ACOM aneurysm with significant Gd uptake demonstrated on T1 (Panel A) and T1+ Gd (Panel B) heatmap reconstructions. Planar 7T-MRI views show minor changes in enhancement, which are not very apparent in 2D views. Based on histogram analysis (Panel C), the aneurysm is GAWE– ($\mu_{\text{post}} < 1$) and SAWE+ ($\mu_{\text{post}} < \mu_{\text{pre}} + 2\sigma$). The survival plot (Panel D) shows that ~82% of spokes enhanced above the SAWE cutoff, and ~2.5% of spokes enhanced above the FAWE cutoff. The circumferential SI of this aneurysm is $\mu_{\text{post}} = 0.70$. SAWE analysis determined that this aneurysm enhances, therefore is at higher risk of rupture (ACOM location, presence of multiple blebs, aspect ratio = 1.68). *GAWE = General Aneurysm Wall Enhancement, SAWE = Specific Aneurysm Wall Enhancement, FAWE = Focal Aneurysm Wall Enhancement

3D Reconstruction



Histogram



Survival Plot

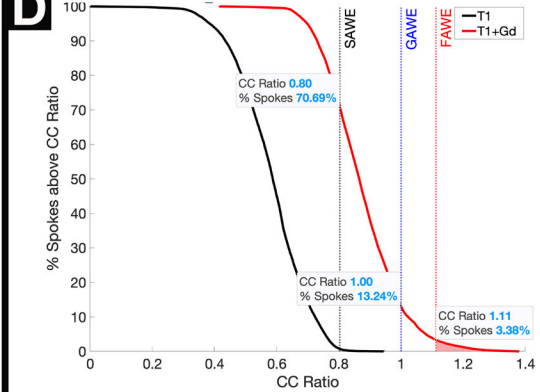
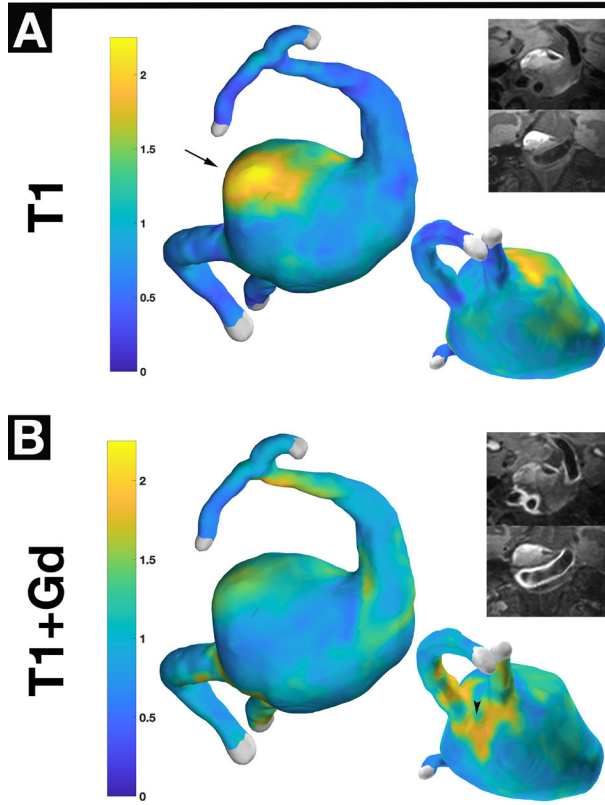
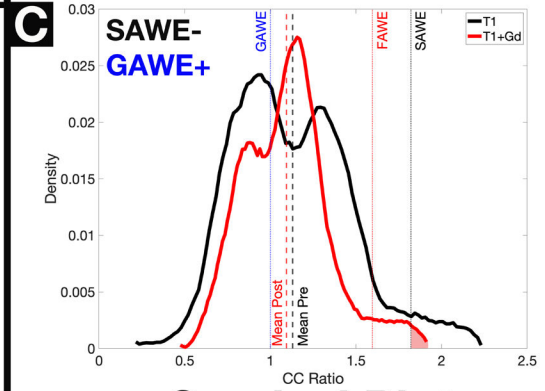


Figure 2. A GAWE⁻/SAWE⁺ fusiform left ICA terminus aneurysm shows no enhancement on T1 (Panel A) and heterogenous enhancement on T1+Gd (Panel B, arrowhead) reconstructions. Despite apparent subjective enhancement from 7T-MRI, this aneurysm is considered GAWE⁻, because only 13% of spokes enhance more than the CC (Panel D). Approximately ~71% of spokes (Panel D) enhance above the SAWE cutoff ($CC_{ratio} = 0.8$); therefore this aneurysm is SAWE⁺. Areas of focal enhancement can be visualized on both the 3D reconstruction (arrow) and 7T-MRI (arrowhead) and are represented in the right tail of the histogram (Panel C). The survival plot (Panel D) shows that the area of focal enhancement comprises only ~3% of the spokes in the aneurysm. This fusiform aneurysm uptakes Gd (SAWE⁺) but is not highly enhancing when compared with other aneurysms (GAWE⁻). Subjective analysis would have classified this aneurysm as enhancing (Panel B, inlet). *GAWE = General Aneurysm Wall Enhancement, SAWE = Specific Aneurysm Wall Enhancement, CC = Corpus Callosum

3D Reconstruction



Histogram



Survival Plot

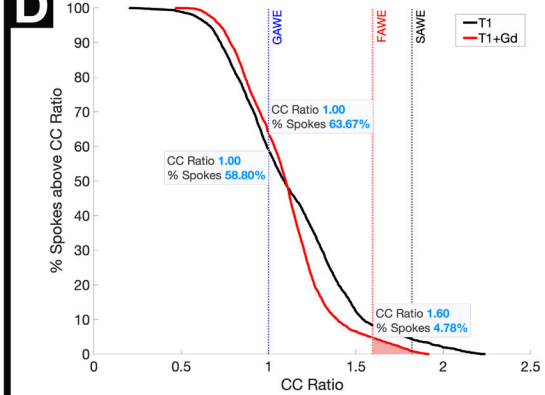


Figure 3. A thrombosed GAWE+/SAWE- verteobasilar aneurysm visualized on T1 (Panel A) and T1+Gd (Panel B) imaging. 7T-MRI shows that the inner wall has avid enhancement compared to the outer layers of the aneurysm sac that encompass the mural thrombus. Areas of focal enhancement on T1 reconstructions (Panel A) are not visualized on T1+Gd reconstructions (Panel B), where new areas of focal enhancement can be visualized. The irregular pattern of enhancement between T1 and T1+Gd is better visualized in the change of histogram shape (Panel C). The survival plot (Panel D) shows that both the T1 and T1+Gd spokes localize above the GAWE threshold (~59% and ~64% respectively). Interestingly, there is more focal enhancement T1 compared to T1+Gd reconstructions, as shown in the survival plot. This case illustrates the complex dynamics of Gd uptake in aneurysms with mural thrombosis. *GAWE = General Aneurysm Wall Enhancement, SAWE = Specific Aneurysm Wall Enhancement

Table 1.

Morphological characteristics of saccular aneurysms with different enhancement patterns.

		Size (mm)	Aspect Ratio	Size Ratio
General Enhancement (N=24)	GAW E+ (N=6)	10.15±6.11	3.73±2.76	3.64±2.57
	GAW E- (N=18)	5.61±2.05	1.91±1.02	1.51±0.62
	p	0.137	0.199	0.104
Specific Enhancement (N=24)	SAWE+ (N=11)	7.96±5.16	2.79±2.36	2.64±2.17
	SAWE- (N=13)	5.71±2.12	2.01±0.96	1.52±0.68
	p	0.424	0.776	0.277
Combined Enhancement (N=24)	GAW E+/SAWE+ (N=6)	10.15±6.11	3.73±2.76	3.64±2.57
	GAW E-/SAWE- (N=13)	5.71±2.12	2.01±0.96	1.53±0.67
	p	0.179	0.244	0.106

* GAW E = General Aneurysm Wall Enhancement, SAWE = Specific Aneurysm Wall Enhancement

Table 2.

AWE of saccular and fusiform aneurysms.

	Saccular (N=24)	Fusiform (N=8)	p
Size (mm) [□]	6.75 ± 3.91	15.3 ± 10.3	0.015
Wall Thickness (mm)	0.527 ± 0.093	0.603 ± 0.083	0.049
Circumferential SI (μ_{post})	0.846 ± 0.246	1.005 ± 0.1937	0.108
% Increase in Circumferential SI ^{□ *}	61.89 ± 41.13	57.47 ± 35.95	0.931
Number of Focal Areas of Enhancement [□]	1.083 ± 0.829	3.378 ± 2.386	<0.001
Area of FAWF (%) [□]	1.82 ± 1.65	4.09 ± 1.07	0.003
Coefficient of Variation (%) [□]	19.5 ± 7.38	24.8 ± 7.26	0.045
Skewness [□]	-0.337 ± 0.881	0.591 ± 0.4225	0.003
Kurtosis [□]	4.39 ± 2.86	3.879 ± 1.207	0.695
SAWE Cutoff	0.8204 ± 0.181	1.0974 ± 0.3448	0.006

[□] Mann-Whitney U significance reported

* % Increase measured from T1 to T1+Gd